Article

The Role of the Second Coordination Sphere of [Ni(PN)](BF) in Reversible Carbon Monoxide Binding

Aaron D. Wilson, Kendra Fraze, Brendan Twamley, Susie M. Miller, Daniel L. DuBois, and M. Rakowski DuBois

J. Am. Chem. Soc., **2008**, 130 (3), 1061-1068 • DOI: 10.1021/ja077328d

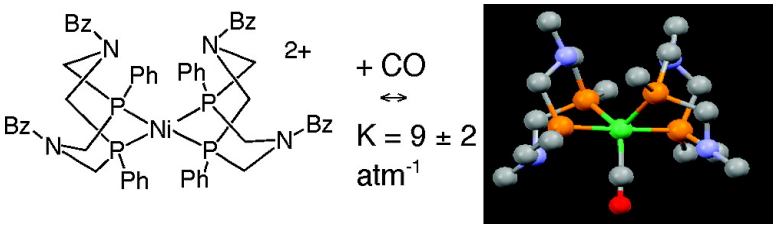

More About This Article

Additional resources and features associated with this article are available within the HTML version:

- Supporting Information
- Links to the 2 articles that cite this article, as of the time of this article download
- Access to high resolution figures
- Links to articles and content related to this article
- Copyright permission to reproduce figures and/or text from this article

View the Full Text HTML

J|A|C|S
ARTICLES
Published on Web 12/29/2007

The Role of the Second Coordination Sphere of $[Ni(P^{Cy}_2N^{Bz}_2)_2](BF_4)_2$ in Reversible Carbon Monoxide Binding

Aaron D. Wilson,[†] Kendra Fraze,[†] Brendan Twamley,[||] Susie M. Miller,[§] Daniel L. DuBois,[‡] and M. Rakowski DuBois*,[‡]

Chemical and Materials Sciences Division, Pacific Northwest National Laboratory, Richland, Washington 99352, Department of Chemistry and Biochemistry, University of Colorado, Boulder, Colorado 80309, Department of Chemistry, Colorado State University, Fort Collins, Colorado 80523, and Department of Chemistry, University of Idaho, Moscow, Idaho 83844

Received September 21, 2007; E-mail: mary.rakowskidubois@pnl.gov

Abstract: The complex $[Ni(P^{Cy}_2N^{Bz}_2)_2](BF_4)_2$, **1**, reacts rapidly and reversibly with carbon monoxide (1 atm) at 25 °C to form $[Ni(CO)(P^{Cy}_2N^{Bz}_2)_2](BF_4)_2$, **2**, which has been characterized by spectroscopic data and by an X-ray diffraction study. In contrast, analogous Ni(II) carbonyl adducts were not observed in studies of several other related nickel(II) diphosphine complexes. The unusual reactivity of **1** is attributed to a complex interplay of electronic and structural factors, with an important contribution being the ability of two positioned amines in the second coordination sphere to act in concert to stabilize the CO adduct. The proposed interaction is supported by X-ray diffraction data for **2** which shows that all of the chelate rings of the cyclic ligands are in boat conformations, placing two pendant amines close (3.30 and 3.38 Å) to the carbonyl carbon. Similar close C−N interactions are observed in the crystal structure of the more sterically demanding isocyanide adduct, $[Ni(CNCy)(P^{Cy}_2N^{Bz}_2)_2](BF_4)_2$, **4**. The data suggest a weak electrostatic interaction between the lone pairs of the nitrogen atoms and the positively charged carbon atom of the carbonyl or isocyanide ligand, and illustrate a novel (non-hydrogen bonding) second coordination sphere effect in controlling reactivity.

Introduction

The development of inexpensive molecular catalysts for the oxidation of hydrogen may ultimately lead to viable replacements for the costly platinum catalysts currently used in hydrogen fuel cells,[1] but few examples of molecular catalysts for this reaction have been characterized.[2,3] We have recently reported that the nickel(II) complex $[Ni(P^{Cy}_2N^{Bz}_2)_2](BF_4)_2$, **1**, serves as a catalyst for the electrochemical oxidation of hydrogen in the presence of a base.[4] Kinetic studies established that the reaction is first order in catalyst and first order in hydrogen, consistent with hydrogen activation being the rate-determining step. The relatively fast rate for this reaction has been attributed to the positioning of two basic sites in the second coordination sphere so that simultaneous interaction of the hydrogen molecule with the metal center and the bases results in a decreased activation barrier for hydrogen oxidation, eq 1.[5]

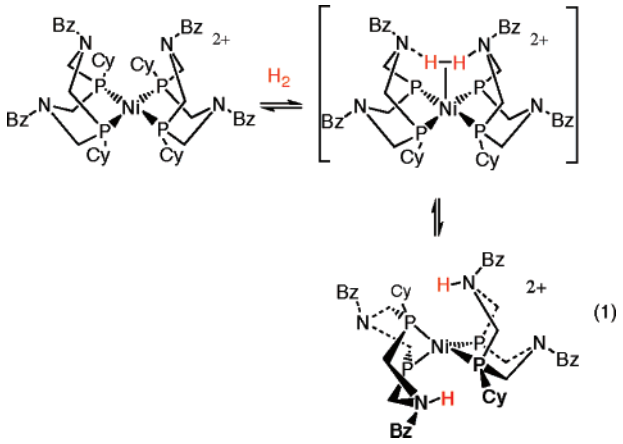

As new molecular catalysts are developed, the opportunity to achieve additional advantages over the platinum catalysts, such as tolerance to carbon monoxide, is also presented. As a result, characterization of the reactivity of **1** with carbon monoxide and its catalytic activity with hydrogen in the presence of CO are of interest. The rapidly developing studies of nickel-containing metalloenzymes that display unusual reactivity with hydrogen or CO provide an additional impetus for studies of synthetic nickel complexes. For example, the nickel−iron hydrogenases, which catalyze hydrogen oxidation/formation, have been found to be inhibited by carbon monoxide.[6,7] In studies of CO with several different oxidation states of the

[†] Pacific Northwest National Laboratory.
[‡] University of Colorado.
[§] Colorado State University.
[||] University of Idaho.

(1) Ralph, T. R.; Hogarth, M. P. *Platinum Met. Rev.* **2002**, *46*, 117.
(2) Collman, J.; Wagenknecht, P.; Hutchison, J.; Lewis, N.; Lopez, M.; Guilard, R.; L'Her, M.; Bothner-By, A.; Mishra, P. *J. Am. Chem. Soc.* **1992**, *114*, 5654.
(3) Curtis, C.; Miedaner, A.; Ciancanelli, R.; Ellis, W.; Noll, B.; Rakowski DuBois, M.; DuBois, D. *Inorg. Chem.* **2003**, *42*, 216.
(4) Wilson, A. D.; Newell, R. H.; McNevin, M. J.; Muckerman, J. T.; Rakowski DuBois, M.; DuBois, D. L. *J. Am. Chem. Soc.* **2006**, *128*, 358.
(5) Wilson, A. D.; Shoemaker, R.; Miedaner, A.; Muckerman, J. T.; DuBois, D. L.; Rakowski DuBois, M. *Proc. Natl. Acad. Sci. U.S.A.* **2007**, *104*, 6951.

enzyme, formation of a paramagnetic nickel(I)−CO adduct has been proposed,[8] and in addition, crystallographic studies have identified a Ni(II)−CO adduct with a bent Ni−C−O bond.[9] The C-cluster of the enzyme CO dehydrogenase (CODH), which catalyzes the two-electron interconversion between CO and CO_2, contains a [Ni−4Fe−5S] cluster at its active site,[10] and mechanisms have been proposed in which the nickel (II) center interacts with the substrates.[11]

Relatively few synthetic nickel(II) complexes containing a carbon monoxide ligand have been reported.[12−19] Examples include anionic complexes such as $[NiCO(SePh)_3]^-$,[12] $[Ni(CO)PS_3]^-$,[13] where PS_3 = tris(3-phenyl-2-thiophenyl)phosphine, and $[NiCO(C_6F_5)_3]^-$,[14] the neutral five-coordinate derivatives $NiI_2(CO)(PMe_3)_2$[15] and $Ni(CO)_3(SiCl_3)_2$[16], and the cationic complex $[NiBr(CO)(PMe_3)_3]^+$.[15] A dicationic five-coordinate complex with a tetradentate phosphine ligand, $[Ni(PP_3)(CO)]^{2+}$, where PP_3 = tris-(2-(diethylphosphino)ethyl)phosphine, has been characterized by an X-ray diffraction study.[17] Extended Hückel studies of ligand characteristics and geometries that may promote the stability of Ni(II)−CO adducts were published several years ago.[17,20] The known Ni(II) structures now include square planar, square pyramidal, and trigonal bipyramidal geometries with CO in both axial and equatorial positions.

This contribution reports our investigations on the reactivity of a series of $[Ni(diphosphine)_2]^{2+}$ derivatives, including $[Ni(P^{Cy}_2N^{Bz}_2)_2](BF_4)_2$, **1**, with an atmosphere of carbon monoxide at room temperature. Complex **1** showed a unique ability to form a CO adduct under these conditions, and further characterization of this product has been carried out. A systematic study of the factors that favor formation of the CO adduct suggest that two bases in the second coordination sphere interact with the coordinated CO ligand to provide a stabilizing influence, and the generality of such an effect in this system is discussed. The effect of carbon monoxide on the catalytic activity of **1** for hydrogen oxidation has also been studied.

Results and Discussion

Survey of $[Ni(diphosphine)_2]^{2+}$ Complexes. A series of bis-(diphosphine) complexes of nickel(II) have been surveyed to assess their reactivity with carbon monoxide (1 atm) at room temperature. The complexes include the previously reported bis derivatives of ligands shown in Chart 1 as well as the following mixed ligand complexes: $[(dppp)Ni(P_2^{Ph}N_2^{Ph})]^{2+}$ and $[(dppm)Ni(P_2^{Cy}N_2^{Bz})]^{2+}$.[3,4,21,22] All of the complexes have been isolated as tetrafluoroborate salts. Two mixed diphosphine dithiolate derivatives, $(dppe)Ni(SC_2H_4S)$[23] and $(PNP)Ni(SC_2H_4S)$[24] were also included in this survey. These complexes were selected to probe the role of the chelate bite size of the bidentate ligands, the electron-donating ability of the substituents on phosphorus, the overall charge on the metal complex, and the role of positioned and nonpositioned pendant amine bases on CO binding.

Chart 1. Diphosphine Ligands and Abbreviations Used in This Study

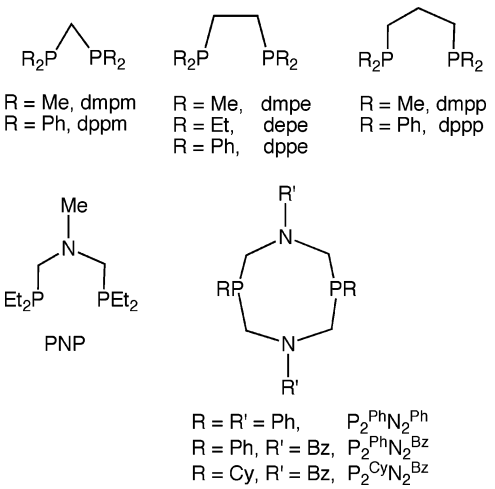

^{31}P NMR spectroscopy was used to monitor the reactivity of each complex with carbon monoxide. Acetonitrile and/or dichloromethane solutions of the complexes were purged with carbon monoxide at room temperature, the NMR tubes were sealed, and spectra were recorded shortly after CO exposure and again after 24 h. An immediate color change and shift in NMR resonances occurred for $[Ni(P^{Cy}_2N^{Bz}_2)_2]^{2+}$, **1**, as described below. None of the other complexes displayed this type of change, and spectra of the starting complexes were observed unchanged after 24 h for all of the other complexes except $[Ni(PNP)_2]^{2+}$. In the case of $[Ni(depe)_2]^{2+}$ the reaction was followed for a much longer time (2 weeks), and no change was observed, implying that these reactions are under thermodynamic rather than kinetic control. In the reaction of $[Ni(PNP)_2]^{2+}$ the ^{31}P NMR spectrum showed evidence for slow formation of a new complex, reaching completion after ca. 24 h.

Reaction of 1 with Carbon Monoxide. Further studies of the reaction of **1** with carbon monoxide were carried out. When an acetonitrile solution of **1** is purged with carbon monoxide at room temperature, a rapid color change from purple to orange is observed. The color change is reversed when the solution is

(6) Lamle, S. E.; Vincent, K. A.; Halliwell, M. L.; Albracht, S. P. J.; Armstrong, F. A. *Dalton Trans.* **2003**, 4152. (b) Lamle, S. E.; Albracht, S. P. J.; Armstrong, F. A. *J. Am. Chem. Soc.* **2004**, *126*, 14899.
(7) Van der Zwaan, J. W.; Coremane, J. M. C. C.; Bouwens, E. C. V. M.; Albracht, S. P. J. *Biochem. Biophys. Acta* **1990**, *1041*, 101.
(8) (a) Stern, M.; Van Lenthe, E.; Baerends, E. J.; Lubitz, W. *J. Am. Chem. Soc.* **2001**, *123*, 5839. (b) Happe, R. H.; Roseboom, W.; Albracht, S. P. J. *Eur. J. Biochem.* **1999**, *259*, 602.
(9) Ogata, H.; Mizoguchi, Y.; Mizuno, N.; Miki, K.; Adachi, S.; Yasuoka, N.; Yagi, T.; Yamauchi, O.; Hirota, S.; Higuchi, Y. *J. Am Chem. Soc.* **2002**, *126*, 11628.
(10) Dobbek, H.; Svetlitchnyi, V.; Liss, J.; Meyer, O. *J. Am. Chem. Soc.* **2004**, *126*, 5382.
(11) Volbeda, A.; Fontecilla-Camps, J. C. *Dalton Trans.* **2005**, 3443.
(12) Liaw, W.; Horng, Y.; Ou, D.; Ching, C.; Lee, G.; Peng, S. *J. Am. Chem. Soc.* **1997**, *119*, 9299.
(13) Nguyen, D. H.; Hsu, H. F.; Millar, M.; Koch, S. A. *J. Am. Chem. Soc.* **1996**, *118*, 8963.
(14) Fornies, J.; Martin, A.; Martin, L. F.; Menjon, B.; Kalamarides, H. A.; Rhodes, L. F.; Day, C. S.; Day, V. W. *Chem.−Eur. J.* **2002**, *8*, 4925.
(15) Saint-Joly, C.; Alain, M.; Gleizes, A.; Dartiguenave, M.; Dartiguenave, Y.; Galy, J. *Inorg. Chem.* **1980**, *19*, 2403.
(16) Janikowski, S.; Radonovich, L.; Groshens, T.; Klabunde, K. *Organometallics* **1985**, *4*, 396.
(17) Miedaner, A.; Curtis, C. J.; Wander, S. A.; Goodson, P. A.; DuBois, D. L. *Organometallics* **1996**, *15*, 5185.
(18) Pierpont, C. G.; Eisenberg, R. *Inorg. Chem.* **1972**, *11*, 828.
(19) Examples of cyclopentadienyl-Ni(II)CO Derivatives: (a) Davidson, J. L.; Sharp, W. A. *Dalton Trans.* **1973**, 1957. (b) Brown, J. M.; Coneely, J. A.; Mertes, K. *J. Chem. Soc., Perkin Trans.* **1974**, *2*, 905.
(20) Macgregor, S. A.; Lu, Z.; Eisenstein, O.; Crabtree, R. H. *Inorg. Chem.* **1994**, *33*, 3616.
(21) Berning, D. E.; Noll, B. C.; DuBois, D. L. *J. Am. Chem. Soc.* **1999**, *121*, 11432.
(22) (a) Fraze, K.; Wilson, A. D.; DuBois, D. L.; Rakowski DuBois, M. *Organometallics* **2007**, *26*, 3918. (b) Fraze, K. Ph.D. Thesis, University of Colorado, Boulder, CO, 2007.
(23) (a) Rauchfuss, T. B.; Roundhill, D. M. *J. Am. Chem. Soc.* **1975**, *97*, 3386. (b) Darkwa, J. *Inorg. Chim. Acta* **1997**, *257*, 137.
(24) Redin, K.; Wilson, A. D.; Newell, R.; Rakowski DuBois, M.; DuBois, D. L. *Inorg. Chem.* **2007**, *36*, 1268.

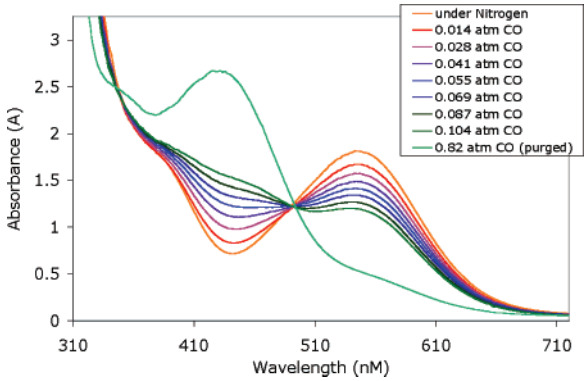

Figure 1. Titration of **1** with carbon monoxide in acetonitrile solution at 21 °C. Each spectrum was recorded after stirring the solution for 1 h to permit equilibration.

purged with nitrogen or evacuated, indicating a reversible binding of carbon monoxide. Figure 1 shows the changes in the visible spectrum of **1** as a function of CO pressure, and from these data the equilibrium constant for the reaction of **1** with CO has been determined to be 8.7 ± 2 atm^{-1}. This equilibrium constant can be used to calculate a $\Delta G°$ of −1.3 kcal/mol for carbon monoxide addition to **1** at 21.5 ± 2 °C, using 1 atm of carbon monoxide as the standard state.

When a solution of the carbon monoxide adduct [Ni(CO)-($P^{Cy}_2N^{Bz}_2$)$_2$](BF$_4$)$_2$, **2**, is purged with CO until solvent has almost evaporated, **2** can be isolated as an orange solid that is stable to air and CO dissociation for a limited time. The infrared spectrum of the solid, recorded on a KBr pellet, shows a strong absorbance at 2063 cm^{-1} for the coordinated CO ligand. In dichloromethane solution a strong band is observed at 2056 cm^{-1} with a shoulder at 2070 cm^{-1}. In the cyclic voltammogram of **2**, recorded in 0.2 M NBu$_4$BF$_4$ benzonitrile solution under a CO atmosphere, two reversible reduction waves are observed at −0.85 and −1.32 V. The small shifts in potentials relative to those observed for the starting complex **1** (−0.80 and −1.36 V) are consistent with the small CO binding constant measured for **1** in acetonitrile. In acetonitrile solution, the Ni(I/0) couple of **2** is accompanied by a stripping wave arising from the poor solubility of the Ni(0) complex in this solvent.

The NMR spectra for **2** recorded in acetonitrile under CO showed broadened resonances at room temperature. In the ^{31}P spectrum two broad resonances are observed at 56 and −4 ppm. In acetone-d_6 solution at −90 °C, the spectrum sharpens, and resonances for two isomers are resolved, Figure 2. The major isomer shows an AA′XX′ pattern with resonances at 61.5 and 1.4 ppm. A minor isomer (approximately 30%) shows four multiplets (ddd) at 63.8, 45.9, −15.5, and ca. 1 ppm. Coupling constants are included in the Experimental Section. The data for the major isomer are consistent with a trigonal bipyramidal structure of C_2 symmetry in which each of the diphosphines spans an axial and equatorial position and the CO occupies an equatorial site, e.g., structure **2a**. The data observed for the minor isomer indicate that the symmetry axis has been removed and this is likely to occur by a conformational change in a chelate ring of the cyclic ligand, e.g., structure **2b**.

Reaction of [Ni(PNP)$_2$]$^{2+}$ with CO. The reaction of [Ni-(η^2-PNP)$_2$]$^{2+}$ with carbon monoxide under similar conditions proceeded at a much slower rate than that of **1**. Over a 24 h period the solution color changed from orange to pale yellow,

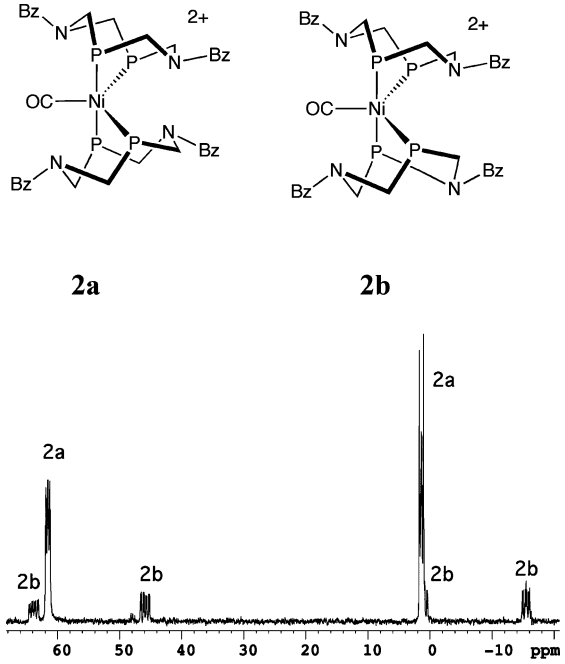

Figure 2. ^{31}P NMR spectrum of **2** recorded on a 400 MHz instrument in acetone-d_6 solution at −90 °C.

and the ^{31}P NMR spectrum indicated that the reaction was nearly complete with the formation of one major new product. The spectroscopic data indicated that the nature of this product was different from that of the CO adduct of **1** and suggest the formation of a nickel(0) complex such as (PNP)Ni(CO)$_2$. Similar reductions of nickel(II) phosphine complexes upon addition of carbon monoxide have been observed previously, although the nature of the reducing agent was not definitively established.[15] In the present system, a dissociated PNP ligand could serve as the reducing agent, but we have not studied this process in detail.

In the PNP system the addition of CO is irreversible, and the starting dication is not recovered upon purging with nitrogen or applying a vacuum. The major resonance observed in the ^{31}P NMR spectrum of the product was a singlet at 17.9 ppm in CD_2Cl_2 (19.9 in CD_3CN), and no change was observed when the spectrum was recorded at low temperature (−90 °C). A solid product, isolated by removal of solvent, showed strong bands assigned to CO stretches in the infrared spectrum at 1941 and 2008 cm^{-1}. The frequencies are similar to those reported previously for Ni(CO)$_2$(PMe$_3$)$_2$ at 1920 and 1990 cm^{-1}.[15] When the cyclic voltammogram of the complex was first scanned in the negative direction, the reversible reduction waves that would be expected for [Ni(CO)(PNP)$_2$]$^{2+}$ were not observed, and upon reversing the scan direction, two irreversible oxidation waves were observed at 0.06 and +0.37 V vs the ferrocene couple. Although a parent peak for an ionized (or protonated form) of Ni(PNP)(CO)$_2$ was not observed in the ESI mass spectrum of the product, a fragment at m/z = 322, corresponding to [Ni-(PNP)(CO)]$^+$ was observed. This fragment was confirmed to be absent in the ESI spectrum of [Ni(PNP)$_2$]$^{2+}$. Although further characterization of this product was not pursued, its properties and spectroscopic data serve to distinguish it from the reversibly formed Ni(II)−CO adduct of **1**.

Evaluation of Reactivity Survey. On the basis of our survey, [Ni($P^{Cy}_2N^{Bz}_2$)$_2$]$^{2+}$, **1**, is unique among the nickel(II) diphosphine complexes in its ability to form a Ni(II)−CO adduct under the

Table 1. Characteristics of Ni(II) Compounds Screened for Reaction with CO

complex	bite angle (deg)	dihedral angle (deg)	$E_{1/2}$ (Ni(II/I))[a]	reaction with CO (solv)
$[Ni(dmpm)_2]^{2+}$	73−74[b]		−1.37	no (CD_3CN)
$[Ni(dppe)_2]^{2+}$	85−86[b−d]		−0.70	no (CD_3CN)
$[Ni(dmpe)_2]^{2+}$	86[d]	3.4	−1.35 (II)/(0)	no (CD_3CN)
$[Ni(depe)_2]^{2+}$	85[d]	0.0	−1.16	no (CD_2Cl_2)
$[Ni(dmpp)_2]^{2+}$	89−94[d]	43.7	−0.89	no (CD_3CN or CD_2Cl_2)
$[Ni(PNP)_2]^{2+}$	90[e]	34.1 (NBu)	−0.64	very slow (CD_3CN or CD_2Cl_2)
$[Ni(dppp)(P_2^{Ph}N_2^{Ph})]^{2+}$	89−94,[d] 80−83[f]		−0.41	no (CD_2Cl_2)
$[Ni(dppm)(P_2^{Cy}N_2^{Bz})]^{2+}$	73−74,[b] 80−83[f]		−0.76	no (CD_2Cl_2)
$[Ni(P_2^{Cy}N_2^{Bz})_2]^{2+}$	83[f]	34.9	−0.80 (−0.66)[g]	yes (CD_3CN or CD_2Cl_2)
$[Ni(P_2^{Ph}N_2^{Ph})_2CH_3CN]^{2+}$	81−83[f]		−0.84 (−0.70)[g]	no (CD_2Cl_2)
$[Ni(P_2^{Ph}N_2^{Bz})_2CH_3CN]^{2+}$	81−83[h]		−0.94 (−0.81)[g]	no (CD_2Cl_2)
$Ni(dppe)(SC_2H_4S)$	85−86,[c] 90[c]			no ($CDCl_3$)
$Ni(PNP)(SC_2H_4S)$	92,[e] 90[c]		−2.34	no (CD_3CN)
$NiI_2(PMe_3)_2$		∼0		yes[i] (CH_3CN)
$NiI_2(PPh_3)_2$		∼90		yes[i] (CH_3CN)

[a] Potentials are reported vs the ferrocene/ferrocenium couple in 0.3 M Et_4NBF_4/acetonitrile at a glassy carbon electrode unless otherwise indicated. [b] Reference 26. [c] Reference 24. [d] Reference 21. [e] Reference 3. [f] Reference 4. [g] These potentials are reported vs the ferrocene/ferrocenium couple in 0.2 M Bu_4NBF_4/dichloromethane. [h] Reference 22a. [i] Reference 15.

conditions studied. There are several interrelated electronic and structural features of this series of complexes that could influence CO binding, including the electron density at the metal center, factors that promote tetrahedral distortions of these nominally square planar complexes, and the potential role of positioned or nonpositioned pendant amine bases.

It is well-known that complexes in which the metal center is relatively electron rich react with carbon monoxide since metal back-bonding into the π^* orbitals of the carbonyl ligand contributes to the stability of the CO adduct. The Ni(II/I) half-wave potential for each of the complexes determined by cyclic voltammetry in acetonitrile solution is indicated in Table 1. The potentials are influenced by electron donor characteristics of the ligand substituents, the ring sizes of the chelating ligands, and the overall charge on the complex. Although a higher coordination number for the metal ion is expected to result in a more negative potential, the potentials of the Ni(II/I) couples in the coordinating solvent acetonitrile and in dichloromethane differ by 0.14 V or less (3.2 kcal/mol). As a result the potentials shown in Table 1 provide a general indication of the electron density at the metal in each complex. It is clear from the data shown in Table 1 that very basic and electron-donating ligands such as dmpm, dmpe, and dmpp do not result in CO binding, and CO binding clearly does not correlate with the Ni(II/I) potential. Even the neutral mixed diphosphine/dithiolate complexes, which have strong pi-donor thiolate ligands and no net positive charge, do not form CO adducts under these conditions.

All of the complexes in this study are diamagnetic and most display approximate square planar geometry. However, it is known that a tetrahedral distortion from the planar structure, indicated by the dihedral angle between the two planes defined by the P−M−P bonds, increases as the chelate ring size increases and as the substituents on the phosphine donor atoms increase in steric bulk. The extent of tetrahedral distortion from a planar geometry has been shown to have a large influence on the binding of hydride ligands,[25] and it is reasonable that this parameter may also influence the binding of CO. Although the natural bite angle of a diphosphine ligand generally correlates with the chelate ring size, the cyclic diphosphine ligands in **1** contain 6-membered chelate rings with an unusually small bite angle of ∼ 80°. Therefore, the reactivity of other nickel diphosphine complexes with small chelate bite angles, e.g., $[Ni(dmpm)_2]^{2+}$, was explored as well as that of other complexes with 5- and 6-membered chelate rings and larger bite angles, e.g., $[Ni(dmpe)_2]^{2+}$ and $[Ni(dmpp)_2]^{2+}$. As shown in Table 1 none of these derivatives formed carbonyl adducts. These results indicate that the bite angle of the ligand is not the dominant factor favoring the binding of CO by **1**.

Despite the small bite angle of the cyclic ligands in **1**, the complex does show a large tetrahedral distortion of 34.9° because of the steric demands of the cyclohexyl substituents on the phosphine donors. However, other nickel complexes with large dihedral angles shown in Table 1, such as $[Ni(dmpp)_2]^{2+}$ (43.7°) and $[Ni(PNP)_2]^{2+}$ (34.1°) did not react in the same way with CO under the same conditions. It therefore does not appear that this tetrahedral distortion is the sole factor in controlling CO binding to these complexes.

Stabilization of the coordinated carbonyl ligand by interaction with one or two nitrogen bases in the second coordination sphere is another possible factor in promoting reaction with CO. Table 1 shows examples of complexes containing the PNP ligand that do not react to form a Ni(II)−CO adduct. In the most stable conformation of the PNP ligand, the amine base is not positioned close to the nickel ion or the potential carbonyl binding site. However, even complexes closely related to **1** containing two cyclic P_2N_2 ligands with *positioned* amine bases, $[Ni(CH_3CN)(P^{Ph}_2N^{Ph}_2)_2]^{2+}$ and $[Ni(CH_3CN)(P^{Ph}_2N^{Bz}_2)_2]^{2+}$, were found to be unreactive with CO. A comparison of the tetrahedral distortion in the cyclic complexes on the basis of X-ray structural data is not possible because the above two complexes crystallize as five-coordinate acetonitrile adducts. However a relationship between the tetrahedral distortion in a $[Ni(diphosphine)_2]^{2+}$ complex and the Ni(II/I) half-wave potential has been discussed previously.[27] The Ni(II/I) half-wave potentials for the three $[Ni(P_2N_2)_2]^{2+}$ complexes recorded in the non-coordinating solvent dichloromethane are included in Table 1. The data indicate that, despite their electron-donating character, the bulky cyclohexyl substituents on the phosphine donors in **1** result in a more

(25) Raebiger, J. W.; Miedaner, A.; Curtis, C. J.; Miller, S. M.; DuBois, D. L. *J. Am. Chem. Soc.* **2004**, *126*, 5502.

(26) Miedaner, A.; Haltwanger, R. C.; DuBois, D. L. *Inorg. Chem.* **1991**, *30*, 417.

(27) For a more detailed discussion of how half wave potentials are influenced by tetrahedral distortions, see ref 22a.

positive half-wave potential corresponding to a significantly larger tetrahedral distortion than is observed for the other cyclic complexes.

It seems likely that the significant tetrahedral distortion of **1** as well as the ability of the pendant nitrogen bases of the diphosphine ligands to interact with CO work together to stabilize the carbonyl adduct, **2**. We propose that the number, positioning, and basicity of the pendant amines in the cyclic diphosphine ligands are all important factors that promote the formation of **2**. The interaction of two pendant bases in **1** with the dihydrogen ligand on nickel has been proposed previously, see eq 1. This second coordination sphere interaction is proposed to decrease the activation barrier for dihydrogen complex formation during the catalytic oxidation of this substrate.[5] This idea is supported by the structure of the first observed product resulting from H_2 activation, $[Ni(P^{Cy}_2N^{Bz}NH^{Bz})_2](BF_4)_2$ (see eq 1), the lower activation barrier of $[Ni(P^{Cy}_2N^{Bz}_2)_2](BF_4)_2$ compared to $[Ni(PNP)_2](BF_4)_2$ for H_2 oxidation, and the results of theoretical calculations, which predict an average N−H distance of 2.40 Å for the N−H−H−N moiety shown in the intermediate in eq 1.[5] Similarly, a structural study of an iron-hydride complex containing a related cyclic diphosphine ligand, *trans*-$[HFe(CH_3CN)(P^{Ph}_2N^{Ph}_2)_2]^+$, shows the close approach of two amine bases to the hydride ligand with an average N−H distance of 2.64 Å[28] compared to the sum of van der Waals radii for N and H of 2.75 Å.[29]

X-ray Diffraction Study of $[(Ni(CO)(P^{Cy}_2N^{Bz}_2)_2](BF_4)_2$, 2. Single crystals of **2** were grown by slow diffusion of carbon monoxide into a dichloromethane solution of **1**, and an X-ray diffraction study was carried out to look for evidence of second coordination sphere effects. In addition to the dicationic nickel complex and two BF_4 anions, the structure includes four noncoordinating dichloromethane molecules. A perspective drawing of the five-coordinate dication is shown in Figure 3a, and selected bond distances and angles are given in Table 2. The complex is a distorted trigonal bipyramid that contains a phosphorus donor from each ligand (P2 and P3) in axial positions with a P2−Ni−P3 angle of 177.7°. The other two phosphorus atoms and the carbon monoxide occupy equatorial positions with the trigonal planar angles ranging from 112.5 to 125.5°. The axial Ni−P distances average 2.21 Å and are slightly shorter than the equatorial Ni−P distances of 2.27 Å. The P−Ni−P bite angles of the two cyclic ligands are similar and average 81.2°. The carbonyl ligand is essentially linear (the Ni−C−O angle = 177.5°) with Ni−C and C−O distances of 1.829(4) and 1.120(5) Å, respectively. The Ni−C distance of 1.83 Å is longer than that of the previously reported dicationic Ni(II) structure (1.78(11) Å)[17] and is on the upper end of the range for all previously reported Ni(II) carbonyls (1.73−1.83 Å).[12−18]

The bond distances and angles for **2** are similar to those determined previously for a related five-coordinate nickel cation with cyclic diphosphine ligands, $[Ni(P^{Ph}_2N^{Ph}_2)_2(CH_3CN)]^{2+}$, **3**, Figure 3b.[4] However a striking difference is observed in the conformations of the six-membered chelate rings of the ligands in **2** and **3**. In **3**, the two six-membered rings closest to the acetonitrile molecule are in chair conformations as might be expected on the basis of steric considerations. In contrast, in **2** all four of the ligand chelate rings are in boat conformations. This arrangement places the pendant amine nitrogens N8 and N56 at distances of 3.30 and 3.38 Å, respectively, from the carbonyl carbon. The distances are slightly larger than the estimated sum of the van der Waals radii for nitrogen and carbon (3.25 Å),[29] but the close approach lends support to the proposal that weak ion−dipole interactions between the partial positive

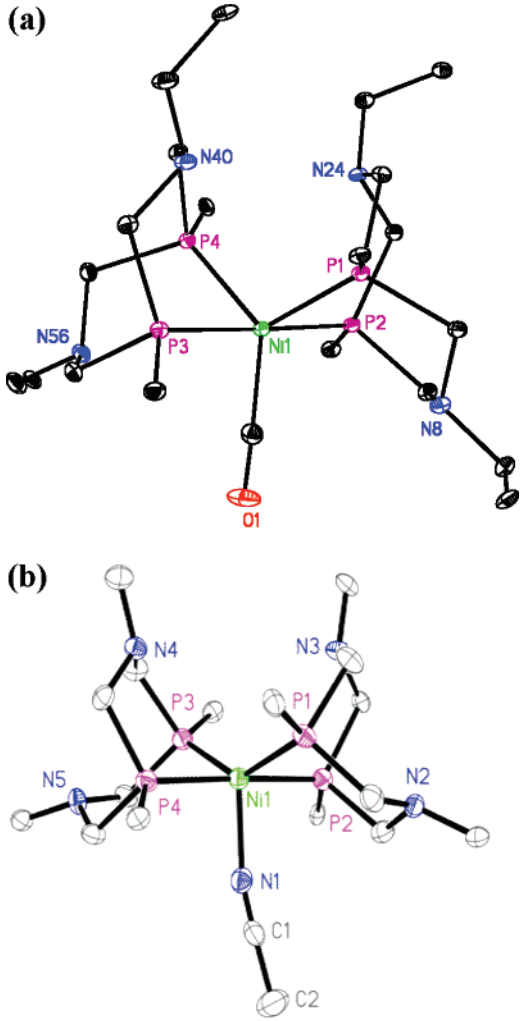

Figure 3. Perspective drawing of (a) the $[Ni(CO)(P^{Cy}_2N^{Bz}_2)_2]^{2+}$ cation of **2**. Thermal ellipsoids are shown at the 30% probability level; (b) the $[Ni(P^{Ph}_2N^{Ph}_2)_2(CH_3CN)]^{2+}$ cation of **3**. For clarity, the drawings show only the carbons of the cyclohexyl and phenyl rings that are directly bound to phosphorus or to methylene carbons of the benzyl substituents in (a) and the ipso carbons of the phenyl groups in (b).

Table 2. Selected Bond Distances and Angles for $[Ni(CO)(P^{Cy}_2N^{Bz}_2)_2](BF_4)_2$, **2**

	bond distances, Å		bond angles, deg
Ni(1)−P(1)	2.2752(10)	P(1)−Ni(1)−P(2)	80.73 (3)
Ni(1)−P(2)	2.2129(10)	P(1)−Ni(1)−P(3)	100.35 (4)
Ni(1)−P(3)	2.2091(10)	P(1)−Ni(1)−P(4)	112.51 (4)
Ni(1)−P(4)	2.2730(10)	P(2)−Ni(1)−P(3)	177.72 (4)
Ni(1)−C(65)	1.829(4)	P(2)−Ni(1)−P(4)	97.12 (4)
O(1)−C(65)	1.120(5)	P(3)−Ni(1)−P(4)	80.62 (4)
		C(65)−Ni(1)−P(1)	121.94 (12)
N(8)−C(65)	3.30	C(65)−Ni(1)−P(2)	91.28 (12)
N(56)−C(65)	3.38	C(65)−Ni(1)−P(3)	89.85 (12)
		C(65)−Ni(1)−P(4)	125.54 (12)
		O(1)−C(65)−Ni(1)	177.5 (4)

(28) Jacobsen, G. M.; Shoemaker, R. K.; McNevin, M. J.; Rakowski DuBois, M.; DuBois, D. L. *Organometallics* **2007**, *26*, 5003.
(29) Douglas, B.; McDaniel, D.; Alexander, J. *Concepts and Models of Inorganic Chemistry*, 3rd ed.; Wiley & Sons: New York 1994; p 102.

Table 3. Selected Bond Distances and Angles for $[Ni(CNCy)(P^{Cy}_2N^{Bz}_2)_2](BF_4)_2$, **4**

	bond distances, Å		bond angles, deg
Ni(1)−P(1)	2.2442(8)	P(1)−Ni(1)−P(2)	81.34 (3)
Ni(1)−P(2)	2.2409(8)	P(3)−Ni(1)−P(4)	81.06 (3)
Ni(1)−P(3)	2.2765(8)	P(1)−Ni(1)−P(3)	112.80 (3)
Ni(1)−P(4)	2.2306(8)	P(2)−Ni(1)−P(4)	177.97 (3)
Ni(1)−C(1)	1.865(3)	C(1)−Ni(1)−P(1)	125.10 (9)
N(1)−C(1)	1.140(3)	C(1)−Ni(1)−P(2)	90.01 (10)
N(2)−C(1)	3.377	C(1)−Ni(1)−P(3)	122.10 (9)
N(5)−C(1)	3.371	C(1)−Ni(1)−P(4)	90.85 (10)
		N(1)−C(1)−Ni(1)	178.7 (3)

charge of the carbonyl carbon and the amine bases promote the formation of the carbonyl complex.

Synthesis of $[Ni(CNCy)(P^{Cy}_2N^{Bz}_2)_2](BF_4)_2$, 4. The reaction of **1** with a bulkier substrate that is isoelectronic with CO, namely cyclohexyl isocyanide, has also been studied. The results of elemental analysis and ESI^+ mass spectrometry on the isolated red product were consistent with the formulation of the expected complex, $[Ni(CNCy)(P^{Cy}_2N^{Bz}_2)_2](BF_4)_2$, **4**. The IR spectrum of **4** shows a C≡N stretch at 2169 cm^{-1}. The ^{31}P NMR spectrum of **4** is similar to that of **2**. At room temperature in acetonitrile-d_3 two broad multiplets at 50.2 and −10.5 ppm are observed. A low-temperature ^{31}P NMR spectrum of **4** obtained at −70 °C in acetone-d_6 shows evidence for two isomers with structures similar to those shown for **2a** and **2b**: an unsymmetrical isomer is assigned to four multiplets centered at 58, 42.2, −5, and −17.9 ppm, and a more symmetrical isomer shows two larger peaks at 56.8 and −5.1 ppm (Figure S1). The sums of the integrals for each isomer indicate a 3:2 ratio of the symmetrical to the unsymmetrical isomer.

X-ray Crystal Structure of $[Ni(CNCy)(P^{Cy}_2N^{Bz}_2)_2](BF_4)_2$, 4. Single crystals of **4** were grown by ether diffusion into an acetonitrile solution. The crystals contained $[Ni(CNCy)(P^{Cy}_2N^{Bz}_2)_2]^{2+}$ cations, BF_4^- anions, and non-coordinating ether (highly disordered) and acetonitrile molecules. Selected bond distances and angles for the dication are given in Table 3, and a perspective drawing is shown Figure 4. As suggested by the spectroscopic data, the coordination geometry of cation **4** is a distorted trigonal bipyramid with the isocyanide ligand in an equatorial position. The structural parameters are very similar to those of **2**. In **4**, the differences between axial and equatorial Ni−P bond distances are less marked, and these bond lengths average 2.25 Å. The Ni−C bond distance of 1.86 Å is slightly longer than that observed for the carbonyl ligand, but the value is similar to those observed for other nickel(II) isocyanide complexes.[14] Space-filling models indicate steric interactions may exist between the isocyanide and diphosphine substituents. However, despite the additional steric bulk of the cyclohexyl-isocyanide ligand, the conformations of the cyclic ligands are similar to those of **2** with all of the six-membered chelate rings in the boat form. The distances between the two nearest nitrogens atoms and the isocyanide carbon (N2−C1 and N5−C1) are 3.32 and 3.41 Å, nearly identical to the N−C distances found for **2**. Once again the close approach to the sum of the van der Waals radii (3.25 Å) suggests that stabilizing interactions exist between the isocyanide carbon and two amines of the second coordination sphere.

Catalytic Activity of 1 in the Presence of CO. Platinum electrodes used for the oxidation of hydrogen in fuel cells are known to be poisoned by trace amounts of carbon monoxide present as a byproduct of H_2 formation from fossil sources. When **1** is used as the catalyst for the electrocatalytic oxidation of hydrogen (1 atm) in the presence of ca. 5% CO, the observed catalytic current was found to be identical to that produced in the presence of pure hydrogen, Figure 5. This CO concentration is much higher than the levels expected in fossil-derived H_2 sources and confirms that the molecular nickel catalyst should be resistant to poisoning by CO, even though it is unique among nickel diphosphine complexes in its ability to form a CO adduct. Comparison of the binding constant for CO addition to **1**, K_{eq} = 8.7 atm^{-1} as determined above, with the previously determined binding constant of 190 atm^{-1} for H_2 addition to **1**[4] indicates that hydrogen addition is favored by a factor of more than 20, and that **1** binds H_2 more strongly than CO by 1.8 kcal/mol.

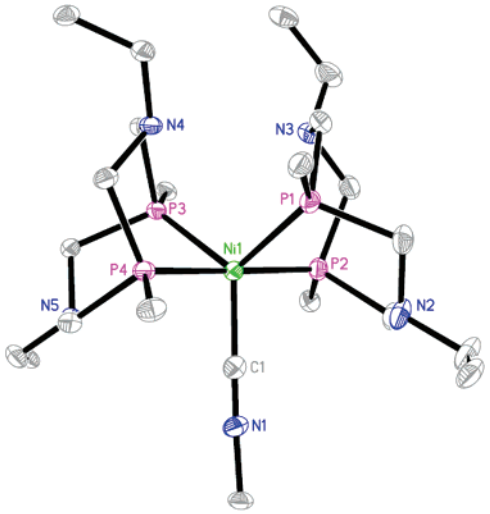

Figure 4. Perspective drawing of the $[Ni(CNCy)(P^{Cy}_2N^{Bz}_2)_2]^{2+}$ cation of **4**. Thermal ellipsoids are shown at the 50% probability level. For clarity, the drawing shows only the carbons of the cyclohexyl and phenyl rings that are directly bound to phosphorus, nitrogen(1) or to methylene carbons of the benzyl substituents.

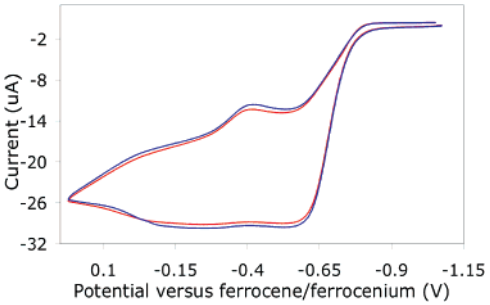

Figure 5. Cyclic voltammogram showing catalytic current for H_2 oxidation for a 1.23 × 10^{-3} M solution of $[Ni(P^{Cy}_2N^{Bz}_2)_2](BF_4)_2$ in the presence of triethylamine (7.2 × 10^{-3} M) under H_2 (ca. 1 atm) (red trace) and under H_2 + 5% CO (ca. 1 atm) (blue trace). Conditions: scan rate = 200 mV/s, acetonitrile solvent, 0.3 M NEt_4BF_4 as supporting electrolyte, glassy carbon working electrode.

Summary and Conclusions

The studies described above indicate that $[Ni(P^{Cy}_2N^{Bz}_2)_2]^{2+}$ rapidly and reversibly binds CO in the Ni(II) oxidation state. In this regard, this complex is unique among the many Ni(II) diphosphine derivatives considered in this study. A systematic study of a series of related complexes suggest that a complex

interplay of electronic and structural factors contribute to this unique reactivity, with an important contribution being the ability of two positioned amines in the second coordination sphere to act in concert to stabilize the CO adduct. This interaction is supported by crystallographic studies of both carbonyl and isocyanide adducts, and it is attributed to an electrostatic interaction between the lone pairs of two nitrogen atoms and the positively charged carbon atom of the bound carbon monoxide or isocyanide ligand. We have reported previous examples of hydrogen-bonding interactions with amines in the second coordination sphere in complexes with the cyclic diphosphine ligand systems. However, the derivatives reported here illustrate that the two positioned pendant bases in the second coordination sphere can stabilize ligands other than dihydrogen or hydrides and that such stabilization can involve interactions other than hydrogen bonds.

Experimental Section

Materials and Instrumentation. Complex **1** was synthesized according to a published procedure.[4] The syntheses of [Ni(dppp)($P^{Ph}_2N^{Ph}_2$)$_2$](BF$_4$)$_2$ and [Ni(dppm)($P^{Cy}_2N^{Bz}_2$)$_2$](BF$_4$)$_2$ have been reported elsewhere.[22b] NMR spectra were recorded on a Varian Inova 400 Mhz spectrometer. ^{1}H NMR chemical shifts are reported relative to tetramethylsilane using residual solvent protons as a secondary reference. ^{31}P NMR chemical shifts are reported relative to external phosphoric acid. All electrochemical measurements were carried out under an N_2 atmosphere in 0.3 M Bu_4NBF_4 in acetonitrile unless stated otherwise. Cyclic voltammetry experiments were carried out on a Cypress systems computer-aided electrolysis system. The working electrode was a glassy carbon disk, and the counter electrode was a glassy carbon rod. A silver wire was used as a pseudoreference electrode. Ferrocene was used as an internal standard, and all potentials are referenced to the ferrocene/ferrocenium couple.

Synthesis of [Ni(CO)($P^{Cy}_2N^{Bz}_2$)$_2$](BF$_4$)$_2$, 2. A solution of [Ni($P^{Cy}_2N^{Bz}_2$)$_2$](BF$_4$)$_2$ (0.20 g, 0.16 mmol) in CD_3CN or acetone-d_6 was purged with carbon monoxide for ca. 15 min. The solution color changed almost immediately from purple to orange. NMR and CV characterization data were obtained under a CO atmosphere for the complex formed in situ. Evaporation of the solvent under a CO atmosphere yielded an orange solid. IR (cm^{-1}) KBr: 2063, (ν_{CO}); In CH_2Cl_2: 2056 (s), 2070 (sh). ^{31}P NMR (CD_3CN, 20 °C): δ 56 (br s); −4 (br s). ^{31}P NMR (acetone-d_6, −90 °C) δ: Isomer 1 (70%): 61.5 (dd, $^2J_{PP}$ = 46 Hz, $^2J_{PP}$ = 57 Hz); 1.4 (dd, $^2J_{PP}$ = 46 Hz, $^2J_{PP}$ = 57 Hz). Isomer 2 (30%): 63.8 (ddd, $^2J_{PaPy}$ = 29 Hz, $^2J_{PaPx}$ = 74 Hz, $^2J_{PaPb}$ = 141 Hz); 45.9 (ddd, $^2J_{PbPx}$ = 22 Hz, $^2J_{PaPy}$ = 74 Hz, $^2J_{PbPa}$ = 141 Hz); ca. 1 (three resolved peaks, $^2J_{PxPb}$ = 22 Hz, $^2J_{PxPa}$ = 74 Hz); −15.5 (ddd, $^2J_{PyPa}$ = 29 Hz, $^2J_{PyPb}$ = 74 Hz, $^2J_{PyPx}$ = 95 Hz). ^{1}H NMR (CD_3CN, 20 °C): δ 7.4 (broad m, 12.6 H); 7.2 (broad m, 8.4 H); 3.8 (broad s, 4.0 H); 3.6 (broad s, 4.5 H); 3.2 (broad s, 4.4 H); 2.4 to 3.0 (broad s, 10.9 H); 1.9 (beneath solvent peak up to 19 H); 1.85 (broad m, 8.2 H); 1.7 (broad m, 10.0 H); 1.1 to 1.5 (broad m, 10.7 H). ^{1}H NMR (acetone-d_6, −90 °C): δ 7.7 to 6.6 (20.0 H); 4.8 to 2.4 (26.1 H); 2.3 to 1.9 (26.7 H includes solvent peak); 1.9 to −0.4 (38.6 H). CV (V vs Fc$^{0/1}$, (ΔE, mV), PhCN): −0.85 (87); −1.32 (64).

[Ni(CNCy)($P^{Cy}_2N^{Bz}_2$)$_2$](BF$_4$)$_2$, 4. A mixture of [Ni($P^{Cy}_2N^{Bz}_2$)$_2$](BF$_4$)$_2$ (0.100 g, 0.0821 mmol) and cyclohexyl isocyanide (20.0 μL, 0.613 mmol) in acetonitrile (15 mL) was stirred at room temperature for 0.5 h to form an orange solution. The volume of the solution was reduced to approximately 5 mL, and ether was added. The solution was placed in a freezer overnight, and the resulting red-orange crystalline solid was isolated by filtration (0.058 g, 53%). Anal. Calcd for $C_{67}H_{99}P_4N_5B_2F_8Ni$: C, 60.47; H, 7.50; N, 5.26. Found: C, 60.65; H, 7.48; N, 5.04. ^{1}H NMR (CD_3CN): δ 7.44 (m), 7.34 (m), 7.27 (m), 7.17 (m) (20H total, PC_6H_5); 3.97 (m, 1H, CNC*H*); 3.83 (broad d), 3.62 (m), 3.42 (m, obscured by ether resonance), 3.32 (m) (8H total, NCH_2Ph); 3.04 (m), 2.86 (m), 2.62 (m) (12H total, PCH_2N, 16H expected); 2.26−1.09 (m, partially obscured by ether resonance) (56H total, PC_6H_{11}, 54H expected). ^{31}P NMR (CD_3CN, room temp): δ 50.22 (m); −10.53 (m). ^{31}P NMR (acetone-d_6, −70 °C): δ approximately 58 (m); 56.78 (m); 42.28 (m); approximately −5 (m); −5.07 (m); −17.97 (m). ESI$^+$ (CH_3CN): *m*/*z* 1242 {[(CyNC)Ni ($P^{Cy}_2N^{Bz}_2$)](BF$_4$)}$^+$. IR (KBr pellet): 2169 cm^{-1}. CV (NEt_4BF_4 in CH_3CN at a scan rate of 200 mV/s): E_p, V vs ferrocene = −1.34 (a stripping wave is observed on the reverse scan).

Determination of Binding Constant for CO Addition to 1. Aliquots of carbon monoxide were added via a gastight syringe to a round-bottom flask (487 mL total volume) containing 4 mL of a 6.90 mM solution of [Ni($P^{Cy}_2N^{Bz}_2$)](BF$_4$)$_2$ in acetonitrile. The flask was fitted with a 2 mm quartz cuvette to permit UV−vis spectral measurements and a sidearm with a gastight septum for introducing gas samples. After addition of each aliquot of CO, the solution was stirred for 1 h to allow the contents to come to equilibrium. Spectra were recorded after equilibration, and the disappearance of the absorbance at 545 nm was monitored (see Figure 1). The last spectrum was recorded after the flask had been purged with carbon monoxide (0.82 atm, ambient pressure in Boulder, CO). The starting absorbance at 545 nm was taken to equal ϵ_1[[Ni($P^{Cy}_2N^{Bz}_2$)](BF$_4$)$_2$], 1340 cm^{-1} M^{-1}. The end absorbance at 545 nm was taken to equal ϵ_2[[Ni(CO)($P^{Cy}_2N^{Bz}_2$)](BF$_4$)$_2$], 400 cm^{-1} M^{-1}. The partial pressure of CO was determined, assuming the volume of CO dissolved in the solution was negligible over the observed pressure range. The equilibrium constant was calculated according to a published method.[30]

X-ray Diffraction Studies. A crystal of **2** was attached to a glass fiber, and data were collected at 90(2) K using a Bruker/Siemans SMART APEX instrument (Mo Kα radiation, λ = 0.71073 Å) equipped with a Cryocool NeverIce low-temperature device. A clear, orange crystal of **4** was mounted on a Mylar loop using Paratone-N oil, transferred to a Bruker AXS Apex2 Kappa CCD, centered in the beam (Mo Kα: λ = 0.71073 Å; graphite monochromator), and cooled to 100(2) K by a nitrogen low-temperature apparatus. Data for **2** were measured using ω scans 0.3° per frame for 20 s, and a full sphere of data was collected. A total of 2400 frames were collected with a final resolution of 0.83 Å. Preliminary orientation and cell constants for **4** were determined by collecting three sets of frames, followed by spot integration and least-squares refinement. A full hemisphere of data was collected using 0.3° ω scans. Cell parameters for **2** were retrieved using SMART[31] software and refined using SAINTPlus[32] on all observed reflections. The raw data for **4** were integrated and the unit cell parameters refined on all data using SAINT. The data for both **2** and **4** were corrected for Lorentz and polarization effects, but no correction for crystal decay was applied. Absorption corrections were applied using SADABS.[33] Structure and solution refinements were preformed (SHELXTL)[34] on F^2 against all reflections. In both **2** and **4**, all non-hydrogen atoms were refined anisotropically and hydrogen atoms were placed in idealized positions, included in structure factor calculations but were not refined. In **2**, two CH_2Cl_2 solvent molecules were disordered, and C14 and C15 were refined in two positions at 83% and 85% occupancy for the major fraction. No decomposition was observed during data collection. Details of the data collection and refinement for **2** are given in Table 1S and for **4** in Table 6S.

(30) Drago, R. S. *Physical Methods for Chemists*; Saunders: New York, 1992; p 99.
(31) *SMART*: v. 5.632; Bruker AXS: Madison, WI, 2005.
(32) *SAINTPlus*: v. 7.23a, Data Reduction and Correction Program; Bruker AXS Inc.: Madison, WI, 2004.
(33) (a) *SADABS*: v. /1, an empirical absorption correction program; Bruker AXS Inc.: Madison, WI, 2004. (b) Sheldrick, G. M. *SADABS*; Bruker Analytical Instruments, Inc.: Madison, WI, 1997.
(34) (a) Sheldrick, G, M. *SHELXTL*: v. 6.14, Structure Determination Software Suite; Bruker AXS Inc.: Madison, WI, 2004. (b) Sheldrick, G. M. *SHELXTL-Plus: A Program for Crystal Structure Determination*, version 5.1; Bruker AXS: Madison, WI, 1998.

Acknowledgment. This work was supported by Grant CHE-0240106 from the National Science Foundation. D.L.D. acknowledges the support of the Office of Basic Energy Sciences of the Department of Energy, by the Chemical Sciences program. The Pacific Northwest National Laboratory is operated by Battelle for the U.S. Department of Energy. The Bruker (Siemens) SMART APEX diffraction facility was established at the University of Idaho with the assistance of the NSF-EPSCoR program and the M. J. Murdock Charitable Trust, Vancouver, WA.

Supporting Information Available: ^{31}P NMR data for **4**, crystallographic data and cif files for **2** and **4**. This material is available free of charge via the Internet at http://pubs.acs.org.

JA077328D